



## GEOSCIENCES

# Retreat of Greenwich, Livingston, Robert and Snow Islands glaciers, Antarctica, between 1956 and 2023

DANIELLE D. SOFFIATTI, KÁTIA K. ROSA, JÚLIA L. LORENZ, FILIPE LINDAU, CARINA PETSCH, FRANCISCO E. AQUINO & JEFFERSON C. SIMÕES

**Abstract:** Glaciers are sensitive to environmental climatic conditions and show their variability over time. This study investigates the environmental characteristics and variation in glacial cover of the Greenwich, Livingston, Robert and Snow islands, Antarctica, between 1956 and 2023. The glacier extension mapping was based on visual interpretation of the Landsat 4, 7 and 8 optical images and normalised difference indexes combination. The REMA 8 digital elevation model was applied to the islands' geomorphometric analysis. Results were compared to climatic series and environmental characteristics. The glacial coverage decreased by 16.9% from 1956 to 2023, equivalent to  $209.95 \pm 0.113 \text{ km}^2$ . Snow Island, with shallow bathymetry near glacial margins and land-terminating ice-fronts, exhibited the smallest retreat rate values. The glacial coverage of Livingston Island decreased significantly (18%, equivalent to  $153.2 \pm 0.113 \text{ km}^2$ ) from 1956-2021, representing the highest values in the study. The changes in glacial coverage of the Robert and Greenwich islands were more substantial in the 1989-2023 period than in 1956-1989. Sectors with marine-terminating glaciers, associated with high bathymetric amplitudes, exhibited more significant variations compared to other sectors, contributing to the evolution of fjord-type bays. Glacial coverage has been lost in recent decades due to regional atmospheric and oceanic warming.

**Key words:** retreat, maritime antarctic region, optical sensors, Landsat, spectral index, spatial temporal analysis.

## INTRODUCTION

The climatology of the Antarctic continent is complex and presents variations, which are the focus of several studies. Turner et al. (2014) recorded atmospheric warming rates of  $0.54^\circ\text{C}/\text{decade}$  in the Antarctic Peninsula (AP) between 1951 and 2011. According to Carrasco et al. (2021), the average temperature increased by  $0.26^\circ\text{C}$  from 1978-2020 in AP.

Tidewater glaciers are complex because their behaviour, dynamics and mass balance are affected by several elements, including climate, oceanic conditions, shape, total precipitation

and surface melting (Cook et al. 2012). Furthermore, the frontal ablation of tidewater glaciers is influenced by wave action and marine surface temperatures (Luckman et al. 2015). The extent of winter sea ice and its annual duration are decreasing in the AP since the 1990s (Smith & Comiso 2008, Hillebrand et al. 2023).

In this context, there is a negative mass balance on King George Island (Michalchuk et al. 2009) and glacial retreat in marine glaciers on this island (Rosa et al. 2023). These factors are related to climate change in recent decades (Smith & Comiso 2008, Hillebrand et al. 2023).

The number of lakes in the South Shetland Islands has increased 60% between 1986/89 and 2000/03 and 55% in 2000/03-2020. The area covered by lakes has grown 52% between 1986 and 2020 (Petsch et al. 2020). Most of the glaciers in the South Shetland Islands are tidewater and have frontal activity with ice calving into the sea. Some areas of the islands present land-, and lake terminating glaciers. Several studies have monitored the retreat and mass balance of the South Shetland Islands glaciers (Cook et al. 2016, Costa et al. 2019, Lorenz et al. 2023). However, there are gaps in estimating glacier areas for different regional sectors and islands. Characteristics of remote sensing tools and products, such as relatively short operating time and the recent and gradual improvement in the spatial resolution of images, are limiting factors in the quantification and analysis of glacier mass loss on a regional and global scale (Hugonnet et al. 2021).

Therefore, this research aims to investigate the variation in the area of the ice caps and ice fields of the Greenwich, Livingston, Robert and Snow islands, Antarctica, between 1956 and 2023. To achieve this aim, we applied spectral indices to optical images to estimate the area variation of ice caps and fields in this period. Annual mean minimum air temperature and precipitation variability were analyzed for the same period. Additionally, we determined the environmental characteristics (area, bathymetry, elevation and slope) of ice caps and fields, with emphasis on the sectors that experienced the most significant decline in the period.

## **MATERIALS AND METHODS**

### **Study area**

The Greenwich, Livingston, Robert and Snow islands are the largest of the South Shetland archipelago with the King George Island, where

the Brazilian Comandante Ferraz Antarctic Station is installed. The South Shetland Archipelago (Figure 1), composed of 29 islands, is located 130 km northwest of AP, between latitudes 61° and 63° 30'S and longitudes 53° 55' and 62° 50'W, between the Drake Strait and the Bellingshausen Sea (Arigony-Neto 2001). The archipelago has an area of 3.740 km<sup>2</sup>. However, only nine islands exceed 100 km<sup>2</sup> (Orheim & Govorukha 1982). The choice of islands is justified as they have an area greater than 100 km<sup>2</sup>, emphasising Livingston Island, the second largest island in the archipelago, with more than 860 km<sup>2</sup>.

### **Delimitation of glacial margins and analysis of environmental parameters**

The glacial margins of Livingston, Snow, Greenwich, and Robert islands were delineated using GLIMS data and the interpretation of optical images from Landsat 4, 7, and 8 satellites, between 1989 and 2023 (Table 1), according to the flowchart presented below (Figure 2). The selected images show little cloudiness and were recorded between December and February (ablation season). There are periods without data due to low availability of suitable images.

The Normalized Difference Snow Index (NDSI) (Crane & Anderson 1984, Dozier 1989) and Normalized Difference Water Index (NDWI) (McFeeters 1996) were applied to satellite images to automatically delimit glacial margins. NDSI (threshold >0.7) was applied to all images to delineate glacial cover. The NDWI (threshold >0.26) was used to extract the NDSI and to remove targets with possible class confusion, such as sea ice, shadows, and small clouds.

Subsequently, the semi-automatic method of identifying the fronts of the ice fields was carried out, based on the products obtained with the spectral indices and subsequent validation with visual interpretation, to get more precise

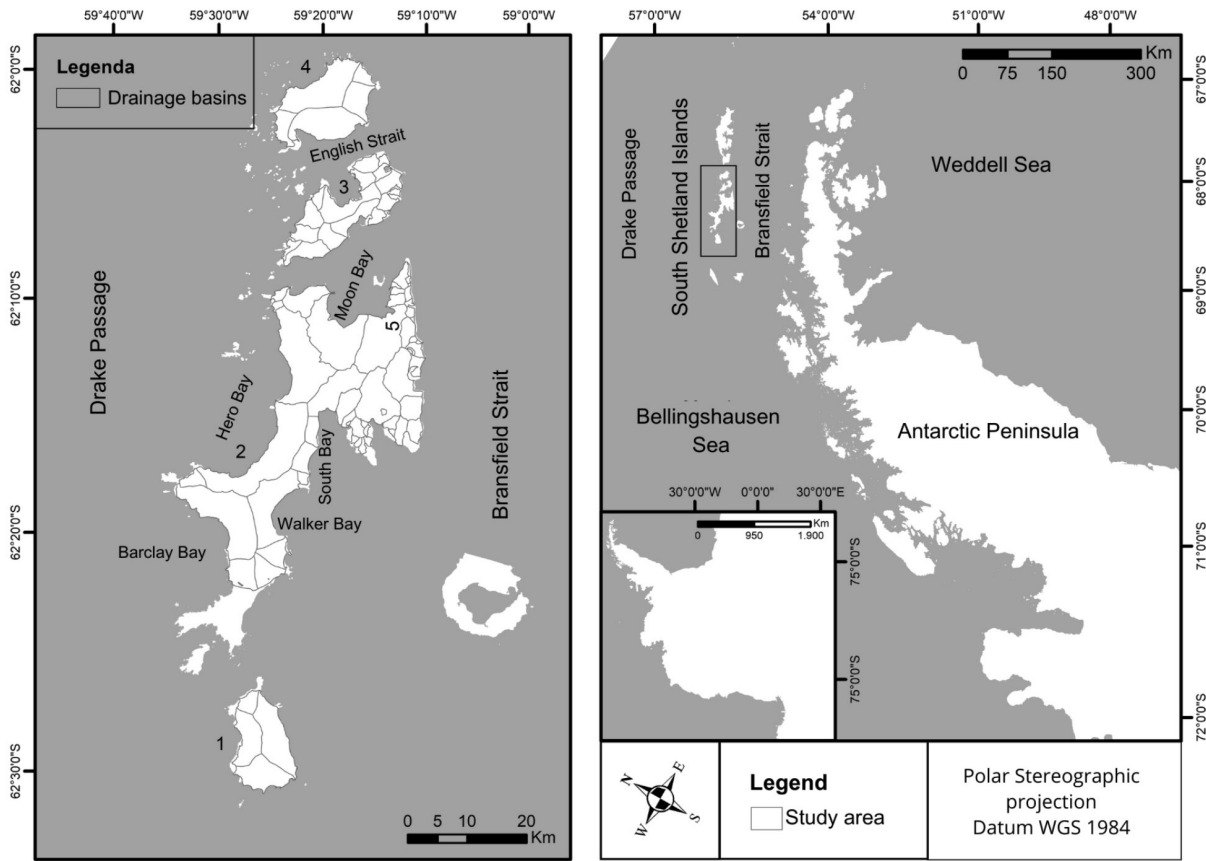


**Figure 1.** Location of study area, South Shetlands, Antarctica. 1: Snow island, 2: Livingston island, 3: Greenwich island, 4: Robert island and 5: Tangra Mountains.

areas of the ice fields and correction of points with class confusion.

The measurement errors of the ice fields by the indices in the images between 1989 and 2021 were quantified and analyzed according to Ye et al. (2006), reference Williams et al. (1997), Hall et al. (2003) and Silverio & Jaquet (2005). Each position has an uncertainty that can be calculated by:

$$Um = \sqrt{\sum \lambda^2} + \sqrt{\sum \epsilon^2}$$

and

$$UA = 2Um \sqrt{\sum \lambda^2} + \sqrt{\sum \epsilon^2}$$

Where *UA* is the glacial area uncertainty, *UT* is the measurement uncertainty of the glacier terminus,  $\lambda$  is the original pixel resolution of each image, and  $\epsilon$  is the registration error, Root Mean Squared Error (RMSE), of each image (Ye et al. 2006).

The RMSE value used was 1.31. This was the result of georeferencing with four control points in the ArcGis software the Landsat 4 image from 1989 based on the Landsat 8 image from 2021. The six Landsat images used have a pixel resolution of 30 m (Table I).

**Table I. Data base. Satellite images and data used in the methodological stage of the study.**

Data/ID	Sensor	Spatial coverage	Acquisition or publication	Spatial resolution	Source
LT04_L2SR_217104_19890128_2020091 7_02_T2	TM	Livingston; Greenwich and Robert	28/01/1989	30 m	<a href="https://earthexplorer.usgs.gov/">https://earthexplorer.usgs.gov/</a>
LE07_L2SR_219104_20020130_2020111 2_02_T2	ETM+	Snow	30/01/2002	30 m	<a href="https://earthexplorer.usgs.gov/">https://earthexplorer.usgs.gov/</a>
LE07_L2SR_217104_20030119_2020091 6_02_T2	ETM+	Robert	19/01/2003	30 m	<a href="https://earthexplorer.usgs.gov/">https://earthexplorer.usgs.gov/</a>
LC08_L1GT_218104_2014016_20201016_02_T2	OLI	Livingston; Greenwich; Robert and Snow	16/01/2014	30 m	<a href="https://earthexplorer.usgs.gov/">https://earthexplorer.usgs.gov/</a>
LC08_L2SR_219104_20200209_2020101 6_02_T2	OLI	Snow and Livingston	03/02/2020	30 m	<a href="https://earthexplorer.usgs.gov/">https://earthexplorer.usgs.gov/</a>
LC08_L2SR_217104_20210112_2021030 8_02_T2	OLI	Greenwich and Robert	12/01/2021	30 m	<a href="https://earthexplorer.usgs.gov/">https://earthexplorer.usgs.gov/</a>
Reference Elevation Model of Antarctica (REMA-8)	-	Livingston; Greenwich, Robert and Snow	2018 (publication)	8 m (spatial resolution); 3.5 m (vertical accuracy) (HOWAT et al. 2019)	Polar Geospatial Center
MDE General Bathymetric Chart of the Oceans (GEBCO)	-	Livingston; Greenwich, Robert and Snow	2023 (publication)	15 arc-second	British Oceanographic Data Centre
Drainage basin shapefiles	-	Livingston; Greenwich, Robert and Snow	1956 (Snow) and 1957 (other islands)	-	GLIMS

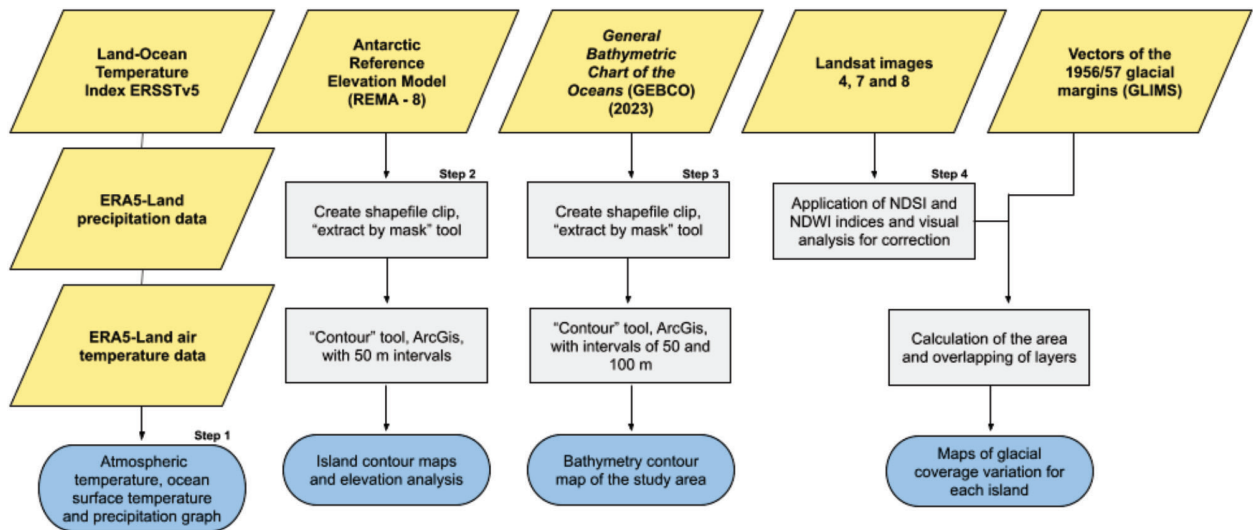


**Figure 2. Research methodological flowchart.**

Hypsometry and area distribution (km<sup>2</sup>) of each island by elevation class were analyzed. The generated products were also visually examined, and the distances between greater depths of the oceanic platform and the margins of the islands were estimated.

The Presidente Eduardo Frei Montalva Station (coordinates -62.19°S, -58.94°W; located 5m above sea level), installed by the Chilean Meteorological Directorate on King George Island, provides temperature data for the period 1989-2021. The Comandante Ferraz Brazilian Antarctic Station (coordinates -62.08°S, -58.39°W; located 5m above sea level), installed by the Instituto Nacional de Pesquisas Espaciais (INPE) on King George Island, provides data for the period 1986-1988. The Polish station Henryk Arctowski (coordinates -62.09°S, -58.28°W; located 2m above sea level), installed in Admiralty Bay, King George Island, provides data for 1977-1985. The method of combining these time series is described in Ferron et al. (2004), and the correlation obtained was  $r > 0.9$ , therefore positive.

The Sea Surface Temperature Anomaly (SST) (°C) average data was obtained by NASA (Land-Ocean Temperature Index ERSSTv5) for 1950-2023 and processed in R software for trend analysis. The annual precipitation data (total and snowfall) and minimum air temperature (1950-2023) for trend analysis of the study area were obtained by ERA5-Land through Google Earth Engine. Temperature values were converted from Kelvin to Celsius, and precipitation values (total and solid) were transformed into centimetres. The data obtained refers to monthly averages. The data has a spatial resolution of 11132 m. ERA5-Land data is produced through reanalysis of European Center for Medium-Range Weather Forecasts (ECMWF) data, which combines observational data with data generated through reanalysis. Other works indicate that for the

northern hemisphere data such as coverage snow images have better accuracy in ERA5-Land than in ERA5 compared to satellite images (Kouki et al. 2023). Regarding air temperature, other studies demonstrate consistency between the data generated by ERA5-Land and observational data (Liu et al. 2021 & Yilmaz 2023). Other studies have already applied ERA5-Land to obtain temperature and total precipitation data on the Antarctic Peninsula (Dirscherl et al. 2021). For the Antarctic continent, a study carried out in McMurdo with field and reanalysis data from ERA5 found that some temperature values do not have such high correlations depending on the season of the year (Girón & Tulaczyk 2024).

## RESULTS

All islands' Icecaps and Icefields exhibited negative variations during the analyzed period (Figure 3a, b). The total glacial area loss was 16.9% ( $209.95 \pm 0.113$  km<sup>2</sup>) from 1956 to 2023 (Figure 3a, b). The glacial area measurements found a maximum error and uncertainty of  $\pm 0.113$  km<sup>2</sup>.

The extent of glacial coverage on Livingston Island decreased from 832.2 km<sup>2</sup> in 1957 to 738 km<sup>2</sup> in 1989, 685 km<sup>2</sup> in 2014 and 679 km<sup>2</sup> in 2020 (Figure 4a), a total area loss of 18.4% ( $153.2 \pm 0.113$  km<sup>2</sup>) (Figure 3b). The retreat rate was 2.4 km<sup>2</sup>/year.

The Icefield of Greenwich Island decreased from 144.9 km<sup>2</sup> in 1957 to 141.2 km<sup>2</sup> in 1989, 131 km<sup>2</sup> in 2014, 127 km<sup>2</sup> in 2021 and 124 km<sup>2</sup> in 2023 (Figure 4b), a loss of area of  $20.9 \pm 0.113$  km<sup>2</sup> or 14.4% (Figure 3a). Its retreat rate was 0.32 km<sup>2</sup>/year.

The glacial coverage of Robert Island decreased from 147.6 km<sup>2</sup> in 1957 to 143 km<sup>2</sup> in 1989, 131 km<sup>2</sup> in 2003, 128 km<sup>2</sup> in 2014, 126 km<sup>2</sup> in 2021 and 122 km<sup>2</sup> in 2023 (Figure 5a). The total area loss of this Icefield was approximately  $25.6 \pm 0.113$  km<sup>2</sup>, equivalent to 17.35%, with a retreat rate of 0.39 km<sup>2</sup>/year (Figure 3a).

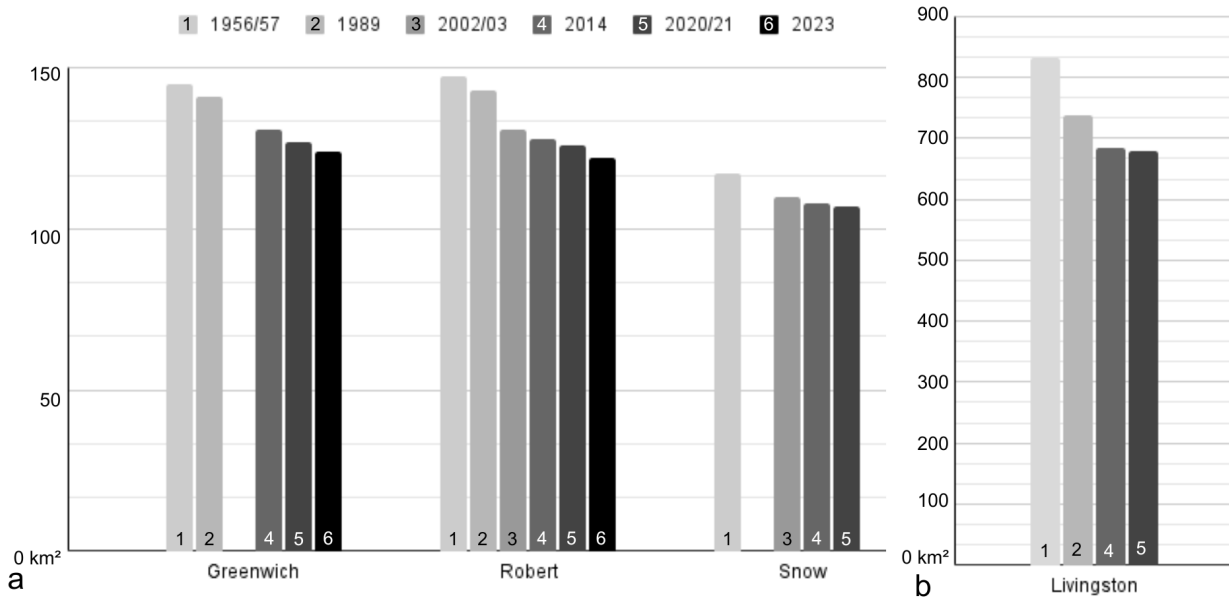


**Figure 3. Variation in the glacier area of the islands between 1956 and 2023. a) Variation in the glaciers area on Greenwich, Robert and Snow islands between 1956 and 2023. b) Variation in the glacier area on Livingston Island between 1956 and 2021.**

The Snow Island’s Icefield area decreased from 117.3 km² in 1956 to 110 km² in 2002, 108 km² in 2014, and 107.04 km² in 2020. The area loss was 10.3 ±0.113 km² (Figure 5b), equivalent to 8.4%, with a retreat rate of 0.16 km²/year, the lowest in the study area (Figure 3a).

Between the periods 1956-1989 and 1989-2021, it is observed that the total area loss of Livingston, Greenwich, and Robert Islands was 8.25%, equivalent to 102.5 km², in the first period, and 7.26%, equivalent to 90.2 km², in the second. Livingston Island, when compared to the others, experienced a more significant loss in the first period, 1956-1989 (11.32% or 94.2 km²), while Greenwich and Robert Islands had more substantial losses in the period 1989-2021 (10.6%, totalling 14.2 km² and 11.89%, totalling 17 km², respectively). The Snow Island was not considered in this analysis because it is not represented in the 1989 image.

Over the last three decades, the annual loss rate for Robert Island since 1989 presented the most significant variations between 1989

and 2002 (0.92 km²/year). The retreat for the subsequent periods (2002-2014 and 2014-2021) was 0.27 km² and 0.28 km²/year, respectively. Snow Island’s area loss rate was 0.17 km²/year between 2002-2014 and 0.14 km²/year between 2014-2021.

Both SST and annual minimum air temperature data showed the highest increases in 1989, reaching 8°C and -7°C, respectively (Figure 6a, b). The data also show similar behaviour in the years 1982 and 2000, showing coherence in the measurements. The annual minimum air temperature between 1950 and 2023 showed variability and a significant increasing trend (Slope = 1304, Z-score = 6.08, p < 0.001) (Figure 6b). The minimum temperature in this series was observed in 1953 (-12.7°C) and 1989 (-6.7°C), with a mean of -9.8°C. The difference between snow precipitation and total precipitation (including liquid) was the greatest in July (Jun = 0.017, Jul = 0.067 and August = 0.006 cm) and the years 1989 and 2016 presented the



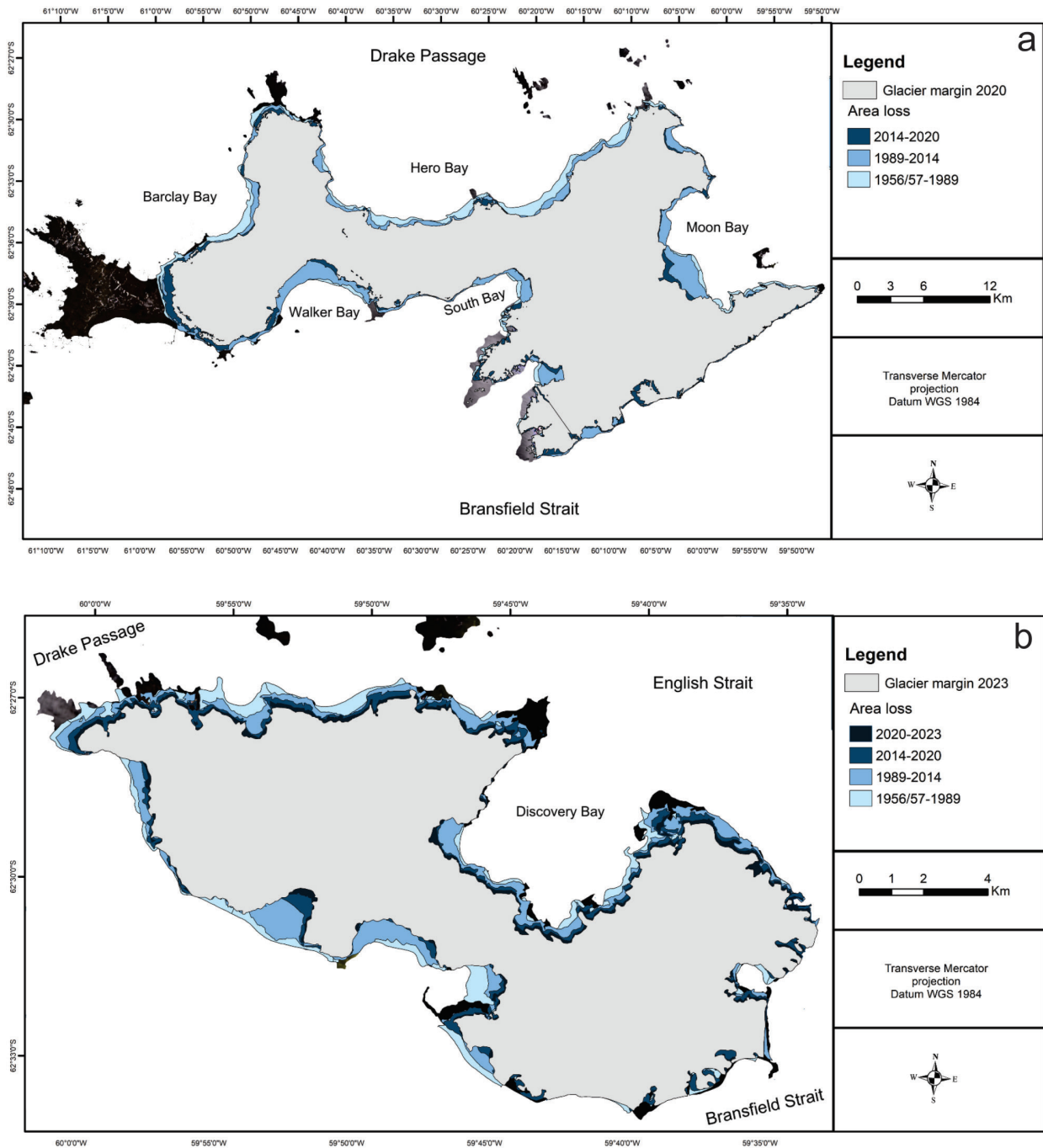


**Figure 4.** Variation in glacial coverage. a) Variation in glacial coverage on Livingston Island between 1956 and 2020. b) Variation in glacial coverage on Greenwich Island between 1956 and 2020.

largest differences between total precipitation and snow values (Figure 6c).

Greenwich, Livingston, Robert, and Snow Islands (Figure 1) have maximum elevations

ranging from 299 to 1.688 m (Figure 7). Livingston Island is the largest island in the study area, with approximately 866 km<sup>2</sup>, with a maximum elevation of 1.688 m (Figure 8a), the highest value

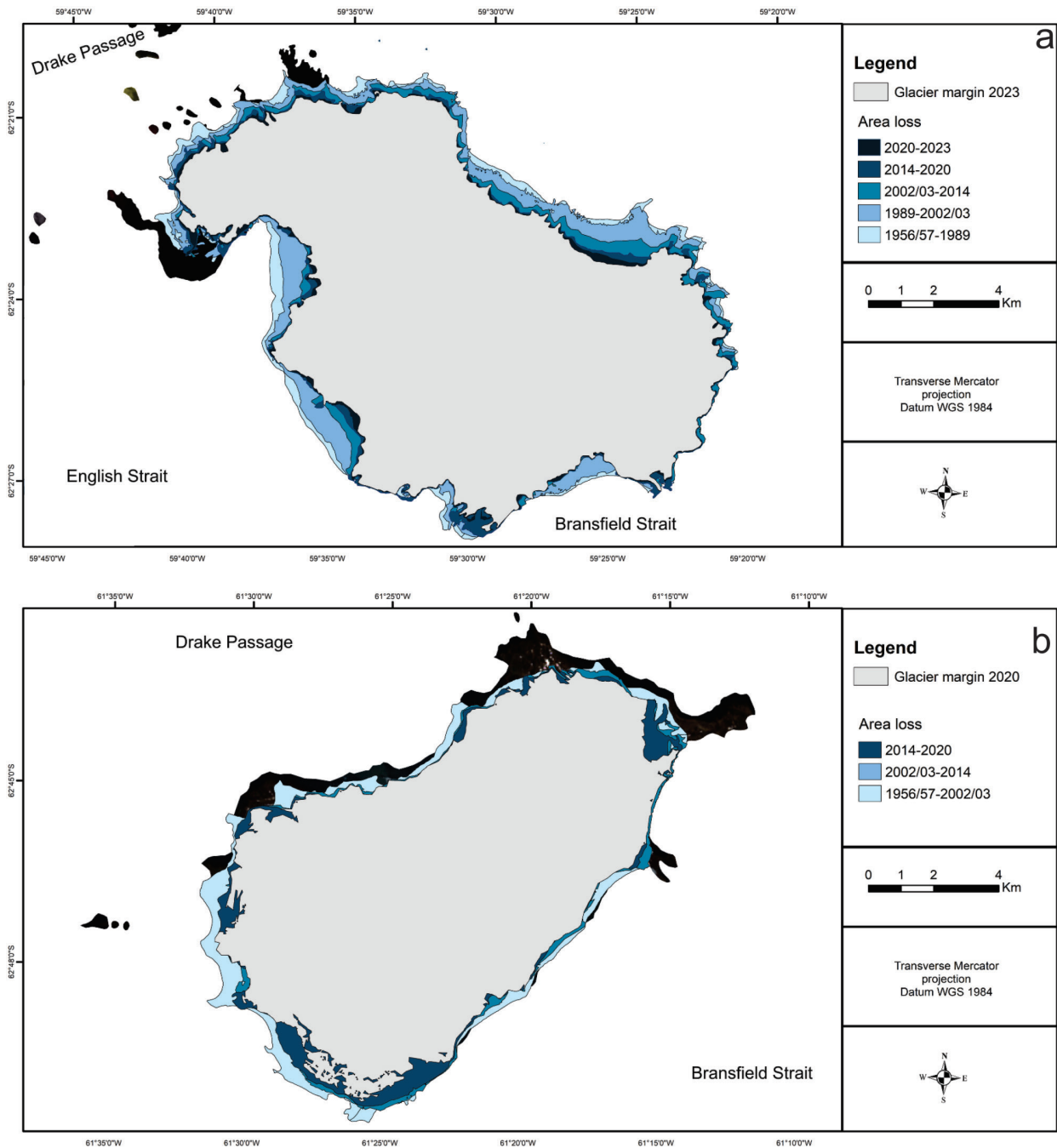


**Figure 5.** Variation in glacial coverage. a) Variation in glacial coverage on Robert Island between 1956 and 2020. b) Variation in glacial coverage on Snow Island between 1956 and 2020.

identified in the study area (Figure 7d). Although approximately 343 km<sup>2</sup> (equivalent to 39.6% of the total area) of the island has values between 0° and 4°, it has the largest area with slopes above 25° (approximately 109.4 km<sup>2</sup>) compared

to the other islands (Table II). The steepest areas are concentrated on the margins of the ice caps and in the southeast portion, where the Tangra mountains are located (Figure 1).



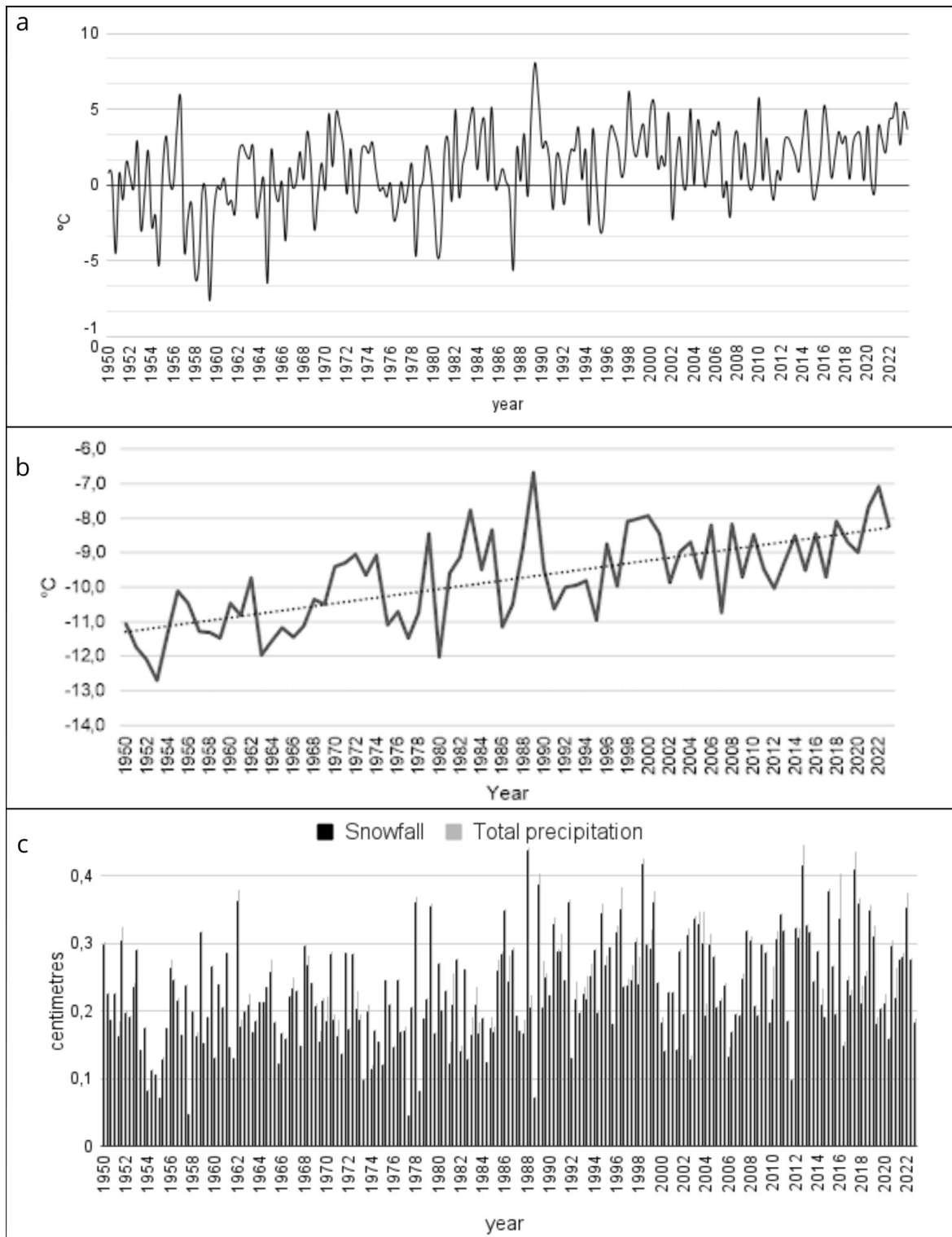


**Figure 6.** Analysis of atmospheric temperature, ocean surface temperature and precipitation. a) Sea surface temperature for the period 1950-2023 in the study area. b) The annual minimum air temperature between 1950 and 2023 in the study area. c) Snowfall and total precipitation for the austral winter (June, July and August) between 1950 and 2023 in the study area.

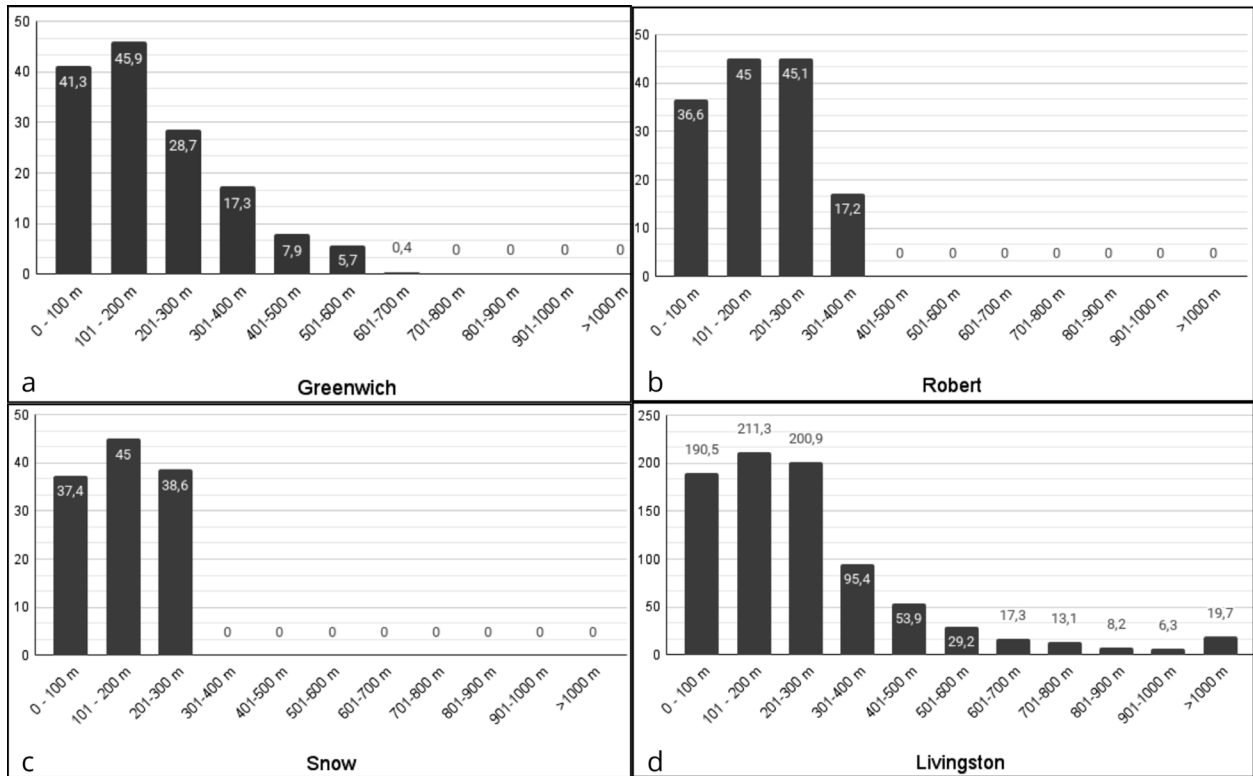


**Figure 7.** Area by elevation class. a) Area (km<sup>2</sup>) of Greenwich Island by elevation class. b) Area (km<sup>2</sup>) of Robert Island by elevation class. c) Area (km<sup>2</sup>) of Snow Island by elevation class. d) Area (km<sup>2</sup>) of Livingston Island by elevation class.

**Table II.** Percentage of total area by slope intervals per island.

Slope	Livingston	Greenwich	Robert	Snow
0° - 4°	39.6%	23.7%	59.6%	59.6%
4,1° - 8°	39.6%	28.9%	25.9%	30.4%
8,1° - 16°	15.6%	27.9%	10.4%	7.5%
16,1° - 25°	7.9%	10.7%	2.3%	1.6%
>25°	12.6%	8.8%	1.8%	0.9%

Greenwich Island is the second-largest island analyzed, covering about 157 km<sup>2</sup> with maximum elevations of 625 m (Figure 7a). The southeast portion of the island also has the highest slope values, with the predominant range between 4° and 8° (Figure 8b), identified in 28.9% (about 45.5 km<sup>2</sup>) of the island’s total area (Table II).

Robert Island covers approximately 150 km<sup>2</sup> and has a maximum elevation of 362.7 metres, concentrated in its central portion (Figure 7b). Most of the areas with steep slopes are located near the coastlines (Figure 9a). Approximately 60% of the island’s extension has slopes between 0° and 4°, indicating a relatively flat relief (Table II).

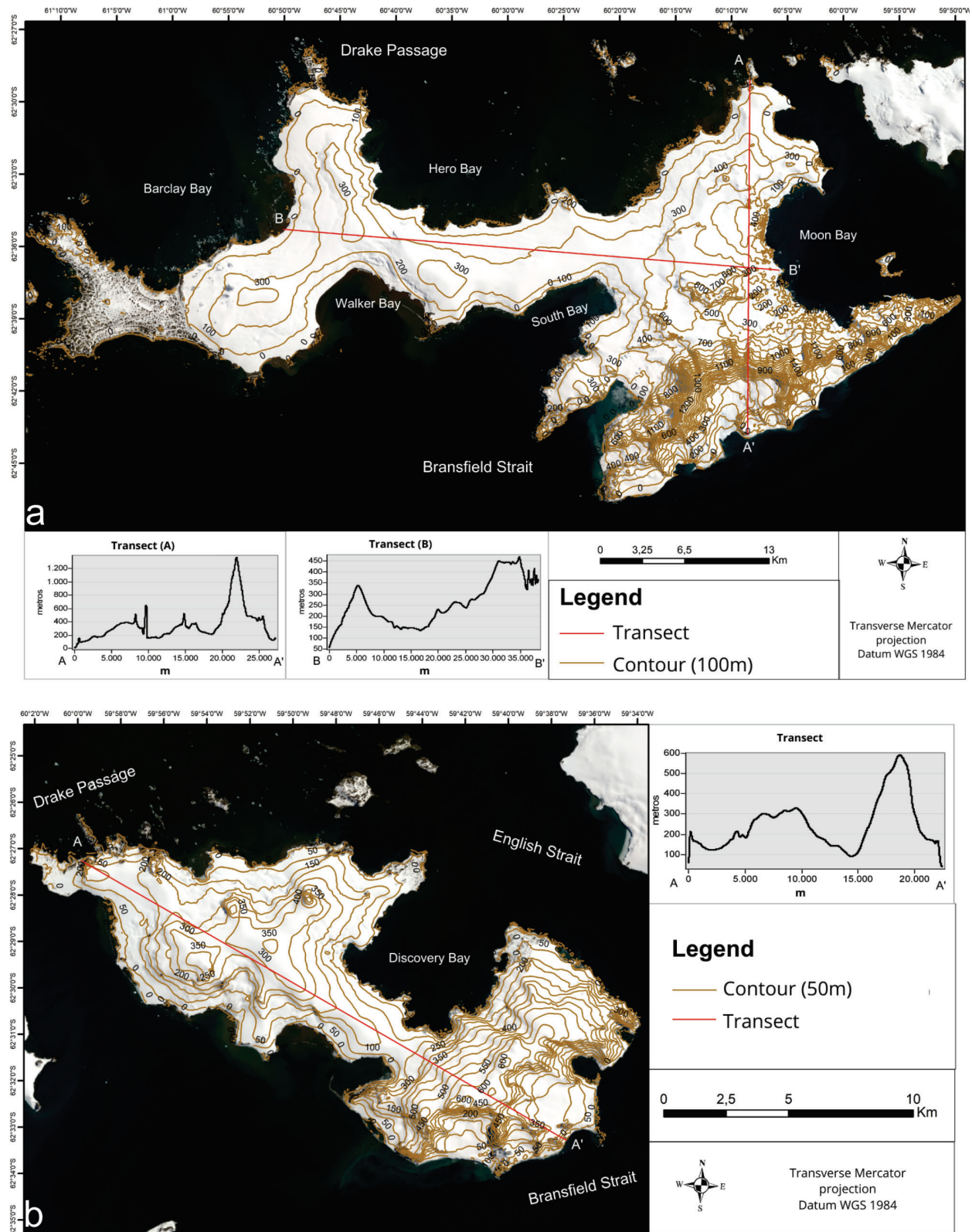
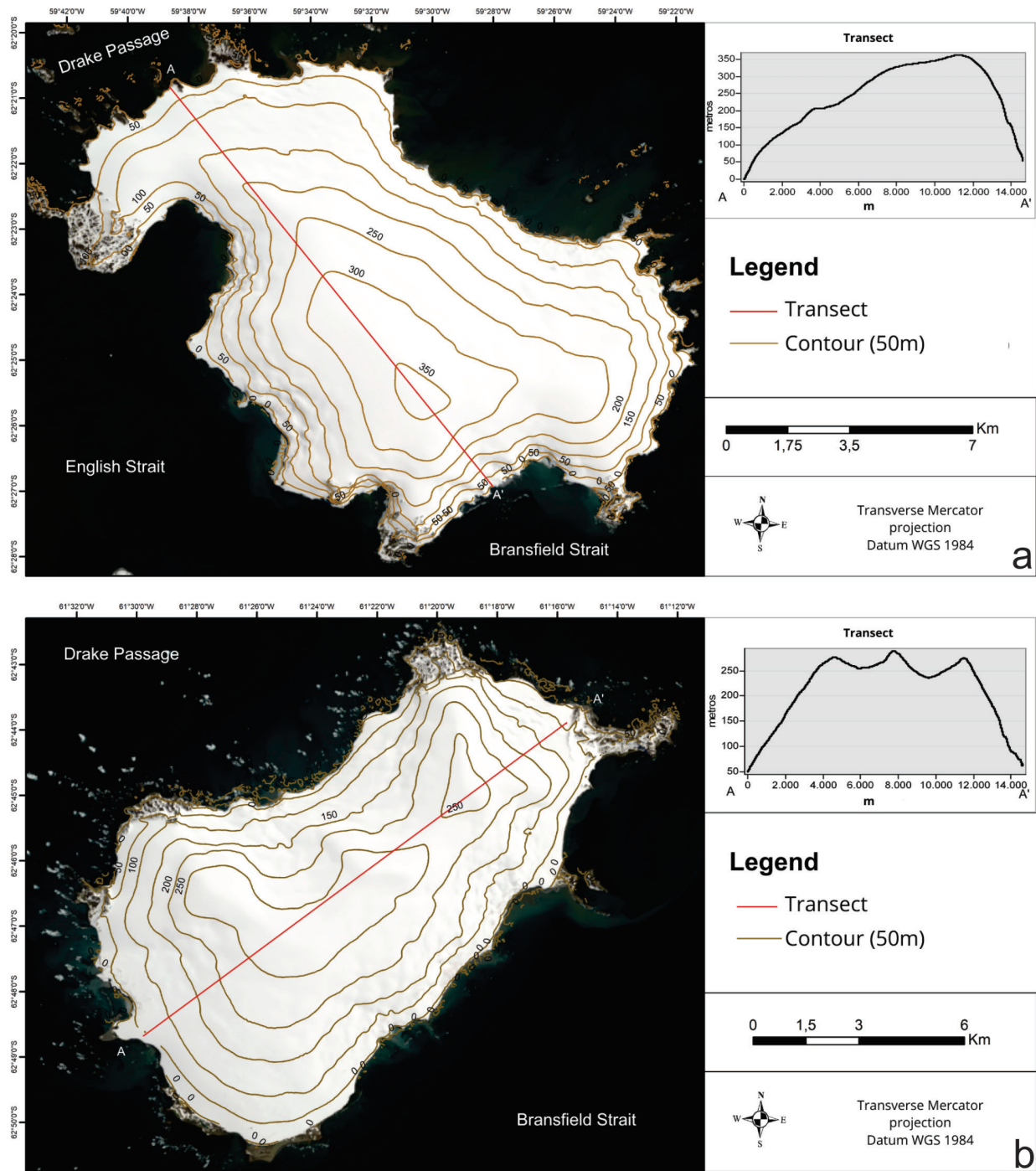


**Figure 8.** Contours and transects. a) Contours and transects of Livingston Island. b) Contours and transect of Greenwich Island.



Snow Island is the smallest in extension, covering 130 km<sup>2</sup> and presenting maximum elevations of 299 metres, distributed in the central area of the island (Figure 7c). Steep

regions are located near the coastline (Figure 9b), with approximately 76.9 km<sup>2</sup> (59.6% of the island's total area) having slopes between 0° and 4°, indicating a relatively flat relief (Table II).



## DISCUSSION

### Retreat of glaciers since 1950 decade and climate variability

Climate change in the region has raised concerns about the sensitivity of sea ice, and this was illustrated by the disintegration of the northern Larsen ice shelves in 1995 and 2002, and flow acceleration and retreat of many calving glaciers in Greenland in the early twenty-first century. Recently, the calving glaciers in Snow, Livingston, Robert and Greenwich Islands showed a high retraction. This process may be related to the negative mass balance and the decreasing thickness at the terminus found in the South Shetlands (Shahateet et al. 2021), which leads to greater sensitivity to atmospheric and sea surface warming trends. Glacier fronts inserted in a context of greater depth in the bays begin to float and may have higher rates of calving, retreat and lead to an acceleration of ice flow (Van der Veen 1998). Where ice is close to flotation, water-filled basal crevasses can penetrate almost through the full thickness of a glacier, potentially leading to calving (Van der Veen 1998).

Furthermore, the sensitivity of the marine glaciers of the islands analyzed, such as Robert Island, is related to the low hypsometric levels, since the summer average temperature is close to the melting point in large portions of the glaciers; therefore, a small temperature change implies a shift from non-melting to melting conditions or vice versa over large areas (Shahateet et al. 2021).

Srivastava et al. (2023) revealed the processes of melting and shrinkage of the Getz Ice Shelf from 2003 to 2019 and found complex interactions between climatic forcings, such as the SST due their significant role in increased basal melting.

The glacial coverage has the lowest area variation in the southeastern region of

Livingston Island, where the highest elevations and slopes are located. Glaciers terminating in the sea and flowing into bays exhibited more significant variations, particularly along the southwest and eastern margins (Figure 4a). The area loss values for Livingston Island (1956-2021) are comparable to those obtained by Cook et al. (2005) for glaciers undergoing more pronounced changes in area loss in the AP (1958-2004). The area loss results for ice caps and ice fields during the period are comparable with studies on King George Island by Lorenz et al. (2023), covering the similar period.

Calvet et al. (1999) reveal a retreat of 0.11%/year for the period 1956-1996 for Livingston Island. The findings in the same area are higher than the author's values. During the period 1956-1989, the annual retreat rate was 2.85 km<sup>2</sup>, equivalent to a loss of 0.34%/year, while the period 1956-2014 had a retreat rate of 2.54 km<sup>2</sup>/year, equivalent to 0.30%/year. Since 1996 was not analyzed in the study, values from the nearest years were used for comparison purposes.

The retreat of glacial coverage on Greenwich Island was more pronounced in the southwest and west portions, in glaciers terminating in the sea, initiating the formation of bays and accentuating existing ones (Figure 4b).

The glacial coverage retreat on Robert Island was more significant in glaciers terminating in the sea, also contributing to the expansion of fjord deglaciation, mainly in the western half of the island (Figure 5a).

The variation in glacial coverage on Snow Island was well-distributed along its margin, showing retreats in all sectors, with the southwest portion, which also has marine glaciers, experiencing visually more significant retreats (Figure 5b).

Regarding the adopted method, the most significant overestimation values, when applying

the automatic method, are found for Livingston Island due to the glaciers terminating on land and with lower slopes containing sediments and supraglacial meltwater. Racoviteanu et al. (2009) state that the NDSI mapping method presents difficulties in regions with clouds, shadows, turbid/frozen/multi-hued proglacial lakes and seasonal snow. Therefore, the visual delimitation methodology is relevant for correcting targets with this class confusion (Racoviteanu et al. 2009). The maximum error and uncertainty of the glacial area measurements in this study are similar to Ye et al. (2006) values ( $\pm 0.042 \text{ km}^2$ ) and are related to 1989 imagery. The measurement errors of the ice fields were also regarded as acceptable as they are comparable to the values obtained by the study used as a reference in this methodological stage (Ye et al. 2006).

When analyzing differences in glacial coverage variation over periods, it is observed that the percentage of area loss calculated since 1957 for Greenwich island (12.3%) is lower than the value of 20.4% found by Fatras et al. (2020). The authors investigated four glaciers on the island flowing from Mount Quito (northwest) and obtained a retreat rate of  $0.27 \text{ km}^2/\text{year}$  for the period 1956-2019. The most significant variation was found in the Quito-I glacier, which terminates in the sea. The differences between the studies are related to land-terminating glaciers in other island sectors, which may exhibit a lower retreat rate than those terminating in water. In the same study, the authors highlight that the El Niño-Southern Oscillation (ENSO) was responsible for increasing the retreat of glacial coverage on the Ambato and Quito-II glaciers in 2015 and 2016. The retreat rates for Greenwich Island for the periods 1989-2014 and 2014-2021 are, respectively,  $0.41 \text{ km}^2/\text{year}$  and  $0.57 \text{ km}^2/\text{year}$ , indicating an increase in the glacial retreat rate after 2014, consistent with the study of Fatras et al. (2020). The more significant glacial

retreat on Greenwich Island in recent years may be related to the behaviour of the minimum temperature that showed an increasing trend from 2016 onwards (Figure 6b).

Between 1989 and 2021, the changes in glacial coverage on Robert and Greenwich Islands were more pronounced. Livingston Island, when compared to the others, experienced a more significant loss in the first period, 1956-1989. The year 1989 had the highest annual minimum air temperatures and SST. Ferron et al. (2004) and Rosa et al. (2020) observed more significant warming for winter in the 1980s when analyzing the time series since 1960 (ERA-5) and 1950 (observational data), respectively. The years 1953-1955, 1958, 1977, 1988 and 2012 have the lowest snowfall and total precipitation values for the austral winter. However the Snowfall and total precipitation showed high variability for the austral winter between 1950 and 2023.

### **The slope and bathymetry as factors contributing to spatial differences in glacial area loss**

The ice caps and ice fields of the Livingston and Greenwich Islands have a larger glacial area distributed in higher elevation classes when compared to others (Figure 8). According to Cook et al. (2005), glaciers with larger front extents generally exhibit more significant mass loss. The distribution of area by elevation controls the accumulation area parameters as well as the accumulation area ratio, which correlates with the mass balance (Oerlemans & Hoogendoorn 1989). Furthermore, shortwave absorption by snow is also influenced by altitude, as the surface albedo significantly decreases in the lower portions of the glacier (Oerlemans & Hoogendoorn 1989), affecting the radiation balance.

The sector with the steepest slopes of the Livingston island ( $>25^\circ$ ) did not exhibit the most significant area losses (Figures 4a and 8a). The



slope class with the most significant area is 0° - 4°, associated with a higher presence of ice-calving glaciers. Regarding glacier slope profiles, Cook et al. (2005) found that glaciers in the accumulation area with low average slope values experienced more significant glacial area loss and are floating-terminus glaciers, this behavior is observed in the study area (Figures 4, 5, 8 and 9).

The greatest variations on Livingston Island are observed for glaciers flowing into bays, such as Walker, South, and Moon Bays (Figure 1), which are fjords characterized by bathymetric amplitudes reaching -250 m (Figure 10). This factor influences the stability of glaciers' grounding lines and flow velocity and has implications for glacial mass balance (Bianchi et al. 2020, Perondi et al. 2023). The decrease

in frontal thickness of marine-terminating glaciers controls the ice-calving rate (Bianchi et al. 2020). Perondi et al. (2023) found greater ice thickness loss in glaciers with steep bathymetric profiles due to increased glacial flow and ice-calving rate. Huybrechts & De Wolde (1999) and Schäfer et al. (2015) assert that ice flow in the ablation zone is intensified by steeper slopes in the frontal sector of glaciers, promoting glacial mass loss. According to Bianchi et al. (2020), fluctuations in the frontal position of tidewater glaciers are influenced by ice-calving, ice flow and basal melt dynamics, and ocean-atmospheric temperature factors. Therefore, the bathymetry of the glacial marine environment and bed topography had controlled the response of tidewater glaciers on Livingston Island to environmental climate changes.

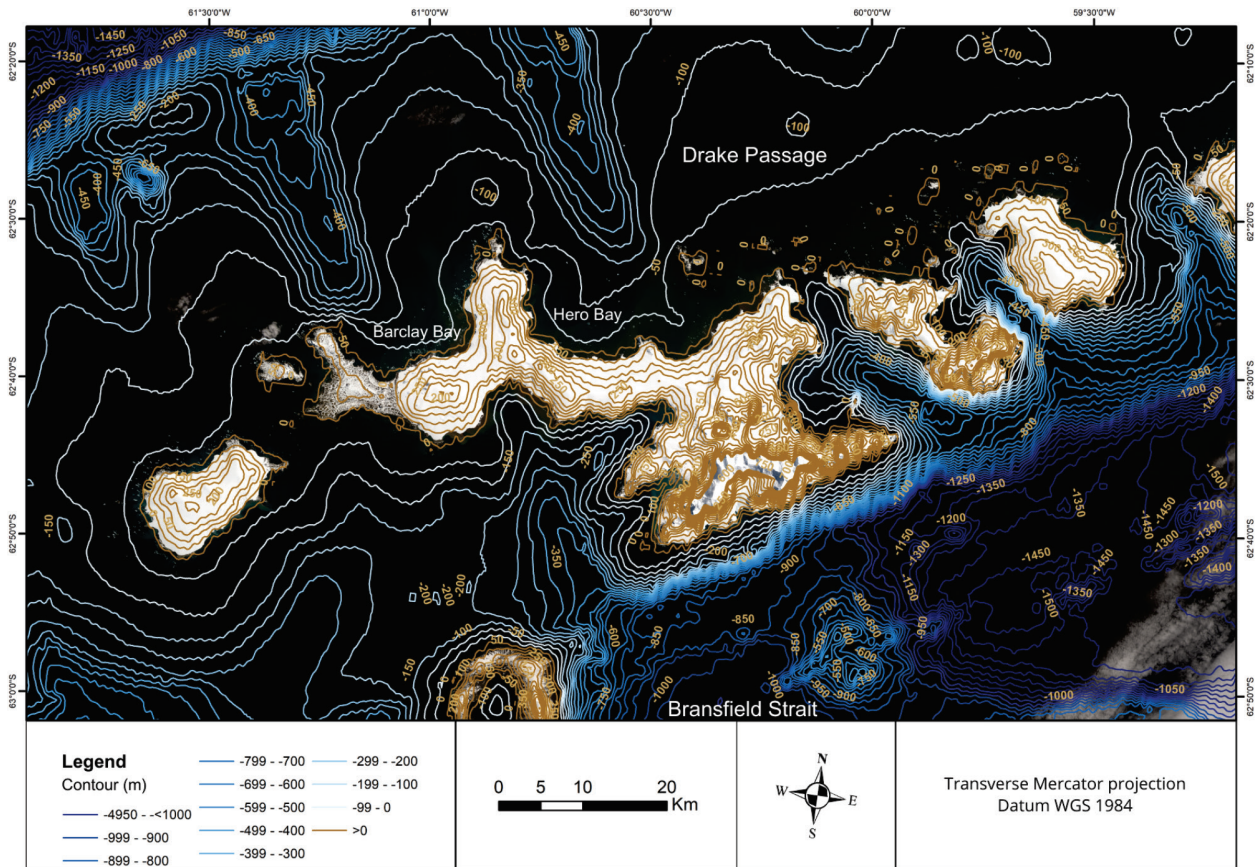


Figure 10. Bathymetric elevation contours in the study area.

The sectors with the highest glacial retreat values on Greenwich Island also correlate with marine-terminating glaciers in sectors with major bathymetric amplitudes (Figures 4b and 10). The western and southeastern sectors of the island are close to depths of -400 m.

Glacial retreat on Robert Island is most significant in the western sector (Figure 5a). Local bathymetric amplitude, reaching depths of -400 m (Figure 10), is higher in this sector and influences glacial dynamics and the response of marine-terminating glaciers to climate change. Hill et al. (2021) state that deeper sectors exhibit greater basal and lateral friction. Marine-terminating glaciers in deeper waters tend to retreat more than those in shallower waters. Snow Island has land-terminating glaciers that are retreating along the entire glacial margin (Figura 5b).

## CONCLUSIONS

Glacier fronts inserted in a context of greater depth in the bays begin to float and may have higher calving and retreat rates and lead to accelerated ice flow. In addition, the sensitivity of marine glaciers on the islands analyzed, such as Robert Island, is related to low hypsometric elevations.

The glacial coverage of Livingston Island has decreased significantly since 1956, representing the highest values in the study. Glacial coverage on Robert and Greenwich islands showed the most significant proportional change from 1989 to 2023, with an accelerated rate of retreat after 2014.

Marine-terminating glaciers on Livingston, Greenwich and Robert islands experienced the most retreat, forming bays and accentuating existing ones. The regional SST warming trend observed is an important factor in changes in the region's glaciers in last decades. The

decreasing area of Icefields and the Icecap represent the negative mass balance of these glaciers, and respond to the increasing minimum air temperature in last decades and the ocean and atmospheric warming trend since the mid-20<sup>th</sup>. The response of the glaciers to behaviour of precipitation in these years needs more investigation.

Sectors with marine-terminating glaciers, associated with high bathymetric amplitudes, exhibited more significant variations compared to other sectors of the islands, contributing to the evolution of fjord-type bays.

The methodology was considered satisfactory, given its ability to encompass automatic measurement through indices and the visual correction of some areas. The cloud coverage and recent snowfall were limiting factors for elaborating the time series with high temporal detail. The NDSI and NDWI indices were efficient for delineating the glacier margin, but occasional visual corrections were necessary due to cloud cover limiting the study's temporal resolution. Combining different satellites and/or using active sensors can provide greater temporal detail. The findings can be useful for continuous monitoring of environmental changes in the area.

## Acknowledgments

We acknowledge the Conselho Nacional de Desenvolvimento Científico e Tecnológico (CNPq), INCT da Criosfera, Brazilian Antarctic Program (PROANTAR), Fundação de Amparo à Pesquisa do Estado do Rio Grande do Sul (FAPERGS) for financial support, and Postgraduate Program in Geography of the UFRGS.

## REFERENCES

ARIGONY-NETO J. 2001. Determinação e interpretação de características glaciológicas e geográficas com sistema de informações geográficas na Área Antártica Especialmente Gerenciada, baía do Almirantado, Ilha Rei George, Antártica. Dissertação de Mestrado, Porto

Alegre: Universidade Federal do Rio Grande do Sul, 84 p. (Unpublished).

BIANCHI TS ET AL. 2020. Fjords as aquatic critical zones. *Earth Sci Rev* 203: 103145.

CALVET J, GARCÍA-SELLÉS D & CORBERÁ J. 1999. Fluctuaciones de la extensión del casquete glaciar de la Isla Livingston, Shetland del Sur desde 1956 hasta 1996. *Acta Geol Hisp* 34: 365-374.

CARRASCO JF, BOZKURT D & CORDERO RR. 2021. A review of the observed air temperature in the Antarctic Peninsula. Did the warming trend come back after the early 21<sup>st</sup> hiatus? *Polar Sci* 28: 100653.

COOK AJ, FOX AJ, VAUGHAN DG & FERRIGNO JG. 2005. Retreating glacier fronts on the Antarctic Peninsula over the past half-century. *Science* 308: 541-544.

COOK AJ, HOLLAND PR, MEREDITH MP, MURRAY T, LUCKMAN A & VAUGHAN DG. 2016. Ocean forcing of glacier retreat in the western Antarctic Peninsula. *Science* 353: 283.

COOK AJ, MURRA YT, LUCKMAN A, VAUGHAN DG & BARRAND N E. 2012. A new 100-m Digital Elevation Model of the Antarctic Peninsula derived from ASTER Global DEM: methods and accuracy assessment. *Earth Syst Sci Data* 4: 129-142.

COSTA RM, PETSCH C, SOTILLE ME, ROSA KK, SIMÕES JC, BREMER UF & ANDRADE AM. 2019. Evidências Geomorfológicas de Mudanças Ambientais na Baía Esperança, Península Antártica. *RDG* 37: 137-149.

CRANE RG & ANDERSON MR. 1984. Satellite discrimination of snow/cloud surfaces. *Int J of Remote Sens* 5(1): 213-223.

DIRSCHERL MC, DIETZ AJ & KUENZER C. 2021. Seasonal evolution of Antarctic supraglacial lakes in 2015–2021 and links to environmental controls. *TC* 15: 5205-5226.

DOZIER J. 1989. Spectral signature of alpine snow cover from the landsat thematic mapper. *Remote Sens Environ* 28: 9-22.

FATRAS C, FERNANDEZ-PALMA BF & MARTILLO C. 2020. Estimating ice retreat on Greenwich island – Antarctica between 1956 and 2019 using optical and SAR imagery. *Polar Sci* 24: 100526.

FERRON FA, SIMÕES JC, AQUINO FE & SETZER AW. 2004. Air temperature time series for King George Island, Antarctica. *Pesqui Antart Bras* 4: 155-169.

GIRÓN RG & TULACZYK SM. 2024. Brief communication: Significant biases in ERA5 output for the McMurdo Dry Valleys region, Antarctica. *TC* 18: 1207-1213.

HALL DK, BAYR KJ, SCHÖNER W, BINDSCHADLER RA & CHIEN JYL. 2003. Consideration of the errors inherent in mapping historical glacier positions in Austria from ground and space (1893-2001). *Remote Sens Environ* 86(4): 566-577.

HILL E, GUDMUNDSSON G, CARR J, STOKES C & KING H. 2021. Twenty-first century response of Petermann Glacier, northwest Greenland to ice shelf loss. *J Glaciol* 67(261): 47-157.

HILLEBRAND F, FREITAS M, BREMER U, ABRANTES T, SIMÕES J, MENDES C, SCHARDONG F & ARIGONY-NETO J. 2023. Concentration and thickness of sea ice in the Weddell Sea from SSM/I passive microwave radiometer data. *An Acad Bras Cienc* 95: 20230342. <https://doi.org/10.1590/0001-3765202320230342>.

HUGONNET R ET AL. 2021. Accelerated global glacier mass loss in the early twenty-first century. *Nature* 592(7856): 726-731.

HUYBRECHTS P & DE WOLDE J. 1999. The dynamic response of the Greenland and Antarctic Ice Sheets to multiple-century climatic warming. *J Clim* 12: 2169-2188.

KOUKI K, LUOJUS K & RIIHELÄ A. 2023. Evaluation of snow cover properties in ERA5 and ERA5-Land with several satellite-based datasets in the Northern Hemisphere in spring 1982–2018. *TC* 17: 5007-5026.

LIU J, HAGAN DFT & LIU Y. 2021. Global Land Surface Temperature Change (2003–2017) and its Relationship with Climate Drivers: AIRS, MODIS, and ERA5-Land Based Analysis. *Remote Sens* 13: 1-20.

LORENZ J, ROSA K, PETSCH C, PERONDI C, IDALINO F, AUGER J, VIEIRA R & SIMÕES J. 2023. Short-term glacier area changes, glacier geometry dependence, and regional climatic variations forcing, King George Island, Antarctica. *An Acad Bras Cienc* 95: 20211627. <https://doi.org/10.1590/0001-3765202320211627>.

LUCKMAN A, BENN D, COTTIER F, BEVAN S, NILSEN F & INALL M. 2015. Calving rates at tidewater glaciers vary strongly with ocean temperature. *Nat Commun* 6: 8566.

MCFEETERS SK. 1996. The use of the Normalized Difference Water Index (NDWI) in the delineation of open water features. *Int J of Remote Sens* 17: 425-4432.

MICHALCHUK B, ANDERSON J, WELLNER J, MANLEY P, MAJEWSKI W & BOHATY S. 2009. Holocene climate and glacial history of the northeastern Antarctic Peninsula: The marine sedimentary record from a long SHALDRIL core. *Quat Sci Rev* 28: 049-3065.

OERLEMANS J & HOOGENDOORN NC. 1989. Mass-Balance Gradients and Climatic Change. *J Glaciol* 35(121): 399-405.

- ORHEIM O & GOVORUKHA LS. 1982. Present-day glaciation in the South Shetland Islands. *J Glaciol* 3: 233-238.
- PERONDI C, ROSA K, MAGRANI F, PETSCH C, VIEIRA R, NETO A & SIMÕES J. 2023. Paleoglaciological reconstruction and geomorphological mapping of Dobrowolski Glacier, King George Island, Antarctica. *Rev Bras Geomorf* 24(3): e2425.
- PETSCH C, ROSA KK, VIEIRA R, BRAUN M, COSTA R & SIMÕES J. 2020. Los efectos de los cambios climáticos en los sistemas glaciales, proglaciales y periglaciales del glaciar Collins, isla Rey Jorge, Antártica, del final de la Pequeña Edad del Hielo al siglo XXI. *Investig Geogr* 103: e60153.
- RACOVITEANU AE, PAUL F, RAUP B, KHALSA SJS & ARMSTRONG R. 2009. Challenges and recommendations in mapping of glacier parameters from space: results of the 2008 Global Land Ice Measurements from Space (GLIMS) workshop, Boulder, Colorado, USA. *Ann Glaciol* 50(53): 53-69.
- ROSA K, PERONDI C, LORENZ J, AUGER J, CAZAROTO P, PETSCH C, SIQUEIRA R, SIMÕES J & VIEIRA R. 2023. Glacier fluctuations and a proglacial evolution in King George Bay (King George Island), Antarctica, since 1980 decade. *An Acad Bras Cienc* 95: 20230624. <https://doi.org/10.1590/0001-3765202320230624>.
- ROSA K, PERONDI C, VEETIL B, AUGER J & SIMÕES J. 2020. Contrasting responses of land-terminating glaciers to recent climate variations in King George Island, Antarctica. *Antarct Sci* 32(5): 398-407.
- SCHÄFER M, MÖLLER M, ZWINGER T & MOORE J. 2015. Dynamic modeling of future glacier changes: mass-balance/elevation feedback in projections for the Vestfonna ice cap, Nordaustlandet, Svalbard. *J Glaciol* 61: 1121-1136.
- SHAHATEET K, SEEHAUS T, NAVARRO F, SOMMER C & BRAUN M. 2021. Geodetic Mass Balance of the South Shetland Islands Ice Caps, Antarctica, from Differencing TanDEM-X DEMs. *Remote Sens* 13(17): 3408.
- SILVERIO W & JAQUET J M. 2005. Glacial cover mapping (1987/1996) of the Cordillera Blanca (Peru) using satellite imagery. *Remote Sens Environ* 95(3): 342-350.
- SMITH WO JR & COMISO JC. 2008. Influence of sea ice on primary production in the Southern Ocean: A satellite perspective. *J Geophys Res* 113: C05S93.
- SRIVASTAVA A, KUMAR A, YADAV J, GUPTA DC & MOHAN R. 2023. Morphological changes and future projections of the Getz Ice shelf, western Antarctica—A statistical and geospatial approach. *Reg Stud Mar Sci* 66: 103144.
- TURNER J ET AL. 2014. Antarctic climate change and the environment: An update. *Polar Rec* 50(3): 237-259.
- VAN DER VEEN CJ. 1998. Fracture mechanics approach to penetration of surface crevasses on glaciers. *Cold Reg Sci Technol* 27(1): 31-47.
- WILLIAMS RS, HALL DK & CHIEN JYL. 1997. Comparison of satellite-derived with ground-based measurements of the fluctuations of the margins of Vatnajökull, Iceland, 1973–92. *Ann Glaciol* 24: 72-80.
- YE Q, KANG S, CHEN F & WANG J. 2006. Monitoring Glacier Variations on Geladandong Mountain, Central Tibetan Plateau, from 1969 to 2002 Using Remote-Sensing and GIS Technologies. *J Glaciol* 52 (179): 537-545.
- YILMAZ M. 2023. Accuracy assessment of temperature trends from ERA5 and ERA5-Land. *Sci Total Environ* 856: 159182.

#### How to cite

SOFFIATTI DD, ROSA KK, LORENZ JL, LINDAU F, PETSCH C, AQUINO FE & SIMÕES JC. 2024. Retreat of Greenwich, Livingston, Robert and Snow Islands glaciers, Antarctica, between 1956 and 2023. *An Acad Bras Cienc* 96: e20240555. DOI 10.1590/0001-3765202420240555.

*Manuscript received on May 30, 2024;  
accepted for publication on September 26, 2024*

**DANIELLE D. SOFFIATTI<sup>1</sup>**

<https://orcid.org/0009-0003-0381-9775>

**KÁTIA K. ROSA<sup>1</sup>**

<https://orcid.org/0000-0003-0977-9658>

**JÚLIA L. LORENZ<sup>1</sup>**

<https://orcid.org/0000-0003-1695-1807>

**FILIFE LINDAU<sup>1</sup>**

<https://orcid.org/0000-0001-7603-7203>

**CARINA PETSCH<sup>2</sup>**

<https://orcid.org/0000-0002-1079-0080>

**FRANCISCO E. AQUINO<sup>1</sup>**

<https://orcid.org/0000-0001-5555-3401>

**JEFFERSON C. SIMÕES<sup>1</sup>**

<https://orcid.org/0000-0001-5555-3401>

<sup>1</sup>Universidade Federal do Rio Grande do Sul, Instituto de Geociências, Centro Polar e Climático, Av. Bento Gonçalves, 9500, 91501-970 Porto Alegre, RS, Brazil

<sup>2</sup>Universidade Federal de Santa Maria, Centro Polar e Climático, Av. Roraima, 1000, 97105-900 Santa Maria, RS, Brazil

Correspondence to: **Danielle Dall Amaria Soffiatti**

E-mail: [danielled.soffiatti@gmail.com](mailto:danielled.soffiatti@gmail.com)

### Author contributions

This manuscript was elaborated by Danielle Soffiatti, with processes optical images. Danielle Soffiatti, Kátia Kellem da Rosa, Júlia Lopes Lorenz, Filife Lindau, Carina Petsch, Francisco Eliseu Aquino, Jefferson Cardia Simões contributed to the writing and revision of the manuscript.

